



A Detailed Assessment of Varying Ejection Rate on Delivery Efficiency of Mesenchymal Stem Cells Using Narrow-Bore Needles

MAHETAB H. AMER, FELICITY R.A.J. ROSE, LISA J. WHITE, KEVIN M. SHAKESHEFF

Key Words. Cell therapy • Mesenchymal stem cells • Differentiation • Needles • Mesenchymal stem cell injection

School of Pharmacy, Wolfson Centre for Stem Cells, Tissue Engineering, and Modelling, University of Nottingham, Nottingham, United Kingdom

Correspondence: Kevin M. Shakesheff, B.Pharm., Ph.D., Centre for Biomolecular Sciences, University Park, Nottingham, NG7 2RD, United Kingdom. Telephone: 0115 9515104; E-Mail: kevin.shakesheff@nottingham.ac.uk

Received August 18, 2015; accepted for publication November 23, 2015; published Online First on January 29, 2016.

©AlphaMed Press
1066-5099/2016/\$20.00/0

<http://dx.doi.org/10.5966/sctm.2015-0208>

ABSTRACT

As the number of clinical trials exploring cell therapy rises, a thorough understanding of the limits of cell delivery is essential. We used an extensive toolset comprising various standard and multiplex assays for the assessment of cell delivery postejction. Primary human mesenchymal stem cell (hMSC) suspensions were drawn up into 100- μ l Hamilton syringes with 30- and 34-gauge needles attached, before being ejected at rates ranging from 10 to 300 μ l/minute. Effects of ejection rate, including changes in viability, apoptosis, senescence, and other key aspects of cellular health, were evaluated. Ejections at slower flow rates resulted in a lower percentage of the cell dose being delivered, and apoptosis measurements of samples ejected at 10 μ l/minute were significantly higher than control samples. Immunophenotyping also revealed significant downregulation of CD105 expression in samples ejected at 10 μ l/minute ($p < .05$). Differentiation of ejected hMSCs was investigated using qualitative markers of adipogenesis, osteogenesis, and chondrogenesis, which revealed that slower ejection rates exerted a considerable effect upon the differentiation capacity of ejected cells, thereby possibly influencing the success of cell-based therapies. The findings of this study demonstrate that ejection rate has substantial impact on the percentage of cell dose delivered and cellular health postejction. STEM CELLS TRANSLATIONAL MEDICINE 2016;5:366–378

SIGNIFICANCE

There are a growing number of clinical trials using mesenchymal stem cells (MSCs) for cellular therapy in a multitude of clinical targets. Numerous cell-therapy procedures use injection-based administration to deliver high-density cell preparations to the target site, either systemically or directly. However, there is growing evidence in the literature of a problem with cell injection methods in various cellular therapy applications. Because a thorough understanding of the limits of cell delivery is essential, an extensive toolset comprising various standard and multiplex assays was used for the assessment of cell delivery post-ejection. The effects of clinically relevant ejection rates and needles were assessed in terms of different aspects of cellular health of ejected human MSCs and their differentiation capacity. Our study emphasizes the potential impact of the administration protocol of cell suspensions and the importance of optimization of delivery parameters according to the nature and cellular responses of cells post-ejection. Our novel findings and comprehensive assessment of different parameters of cellular health and differentiation potential may be used to improve cell delivery using fine needles.

INTRODUCTION

Mesenchymal stem cells (MSCs) have been the focus of numerous preclinical and clinical studies, affording promise in the treatment of various conditions using cell therapy [1–4]. MSCs have been investigated to regenerate damaged tissue resulting from brain and spinal cord injury, myocardial infarction, diabetes, stroke, and bone injuries [5]. However, one of the main translational challenges of cell therapy is the need to determine and achieve suitable delivery protocols of the administered cell dose [6].

MSCs have demonstrated valuable therapeutic potential because of their relatively convenient isolation and multilineage differentiation potential [7], and ability to promote vascularization [8]. However, a major barrier to the implementation of MSC therapy is achieving the required cell dose at the injection site [9]. In addition, the fate of MSCs following systemic infusion is mostly unknown [9]. Cellular therapy procedures use injection-based administration to accurately administer high-density cell preparations, either by direct injection or systemically [10]. However, clinical translation of cellular

therapeutics is hampered by the significant loss of transplanted cells after delivery. Early cell loss has been reported to be observed within the first minutes of implantation [11], with one study quantifying immediate postinjection cell survival at 60% [12], and another found that only 44.8% of cells survived 10 minutes after implantation [13].

There are many challenges to the injectable delivery of fragile cell-based therapeutics, particularly when small volumes of cell suspensions are required to be transplanted with high accuracy. Because numerous cell-therapy procedures necessitate the use of syringe-based delivery devices to directly inject cells, especially in the case of sites of limited accessibility, there is a pressing need for the optimization of injectable cell delivery systems and to understand the influence of the injection process on subsequent cellular functionality. Physicians may favor the use of fine needles to minimize physical damage and patient discomfort, but these may affect cell viability. Additionally, injection protocols mainly depend on trial and error [14]. Therefore, robust cell delivery protocols must be optimized to accelerate translation to the clinic.

To enable clinical translation of cell therapy, research has been carried out to evaluate the impact of injection on cell functionality [15–22]. Nevertheless, the discrepancies in the delivery devices and administration methodologies used has complicated comparisons and led to contradictory results. This is illustrated in some studies that demonstrated that cell manipulation through a needle did not significantly affect viability [16, 17], whereas others stated that it did exert a significant effect [19]. However, it would be misleading to assume the same degree of impact and magnitudes of shear stress were experienced by all cells used, because of differences in sizes and shapes, as well as different needle gauges and syringes used. Another potential concern is the inadequate testing of the many aspects of cellular health in most studies, thereby not providing the complete picture needed to develop appropriate clinical administration protocols. This is evident in some studies that have only relied on the analysis of cell viability to conclude that cells were not affected by the injection parameters under investigation [20–22]. In addition, some studies have used a relatively small sample size ($n \leq 3$) for their investigations [17–19]. Moreover, different studies had different definitions of “effective cell transplantation.” In a study by Kondziolka et al., a reduction of almost 50% in viability of cells postinjection was considered acceptable [23]. On the other hand, the Center for Biologics Evaluation and Research has stated that cellular therapy products should display $\geq 70\%$ viability and a repeatedly high level of potency [24]. However, it does not recommend at what stage, from cell culture to implantation, this level of viability is expected.

In an attempt to improve the number of cells that are successfully delivered to the target site, typical doses used in clinical trials comprise up to hundreds of millions of MSCs [9]. However, no agreement exists regarding the optimal cell number to be transplanted, although this is likely to vary depending on cell type and treatment. Preclinical and clinical studies have explored cell therapies, using a wide variety of administration methodologies, doses, and target organs, resulting in variable outcomes. Some studies have suggested that an increasing cell dose is associated with a better left ventricular ejection fraction improvement in patients with myocardial infarction [25, 26], whereas some have shown an inverse dose response to cell number injected in patients with ischemic cardiomyopathy [27]. Other clinical studies have reported that low cell doses were as effective as higher ones in inducing response [28], with a recent study demonstrating that

a suitable cell dose, rather than a higher one, can better aid the repair of injured tissue in patients who have had a stroke [29]. Moreover, there is a possibility of microembolism with high cell doses in intracerebral transplantations [30]. Therefore, more investigations are required to optimize cell-delivery protocols using minimal cell numbers to achieve enhanced delivery.

Although MSCs have been shown to be safe and effective for a range of cell-therapy applications [31], critical challenges need to be addressed before they are established as a standard of care. With the rising number of clinical trials exploring possible cell-therapy applications using MSCs, understanding factors that may impact the functionality of these cells postinjection is of utmost importance. An enhanced understanding of what happens to cellular therapeutics postinjection, specifically with regard to vital cellular health parameters, will facilitate the development of more efficient administration and formulation approaches to achieve higher efficacy and reduce variability. Following on from our previous work [32], we used a broad toolset for the assessment of cell delivery postinjection to explore the various aspects of administration of primary human MSCs after ejection from clinically relevant, narrow-bore needles.

MATERIALS AND METHODS

Human Mesenchymal Stem Cell Culture

Primary human bone-marrow mesenchymal stem cells (hMSCs) were obtained from Lonza (Cologne, Germany, <http://www.lonza.com>) and cultured in mesenchymal stem cell growth medium (MSCGM) (#PT-3001; Lonza) with 5% CO₂ at 37°C. The lot numbers of hMSC batches obtained from male and female donors were as follows: #0000351482, #0000411107, and #0000422610, and these were cultured as individual patient stocks. Donor characteristics are shown in supplemental online Table 1. These cells were tested for the ability to differentiate into osteogenic, adipogenic, and chondrogenic lineages. All routine passaging and differentiation procedures were performed according to Lonza's Poietics human mesenchymal stem cells protocols. Cells used in this study were between the third to fifth passages.

Preparation of hMSCs and Ejection Protocol

After trypsinization, cells were centrifuged and then reconstituted to a density of 7×10^5 cells per milliliter in phosphate buffered saline (PBS) for cell-ejection studies, unless otherwise stated. Density of suspensions used in this study was selected conservatively based on earlier clinical studies [33–36] as well as practical considerations. Aliquots (100 μ l) of this cell suspension were used for ejection experiments. Cells were directly pipetted into well plates to provide controls (i.e., not ejected through a needle).

For cell ejection, 100- μ l Hamilton GASTIGHT syringes (model 1710RN; Hamilton Bonaduz, Switzerland, <http://www.hamiltoncompany.com>), attached to customized 30G and 34G 20-mm removable stainless steel needles, were used. All flow studies were performed at room temperature. Cell suspensions were drawn up with a Harvard Infuse/Withdraw syringe pump (PHD 2000; Harvard Apparatus, Holliston MA, <https://www.harvardapparatus.com>) at 300 μ l/minute through the needle before being ejected at various rates into Eppendorf tubes. The ejected samples were then transferred into the appropriate well plates. Needle-gauge sizes were chosen to be appropriate for high-accuracy cell-therapy applications. Ejection rates used in this

study (10–300 $\mu\text{l}/\text{minute}$) were selected to mimic clinically relevant ejection while still being practical to use with a syringe pump.

Cell Size, Flow Parameter, and Shear Stress Calculations

Poiseuille's equation was used to calculate shear stress:

$$\tau = \frac{4Q\eta}{\pi R^3} \quad (1)$$

where τ_{max} is shear stress (dyn/cm^2), Q is flow rate (cm^3/s), η is dynamic viscosity of the medium (PBS treated as water at room temperature; $0.01 \text{ dyn} \times \text{s}/\text{cm}^2$), and R is needle radius (30-gauge [30G] internal radius = $7.9 \times 10^{-3} \text{ cm}$; 34-gauge [34G] internal radius = $2.55 \times 10^{-3} \text{ cm}$) (Table 1).

Transit time was calculated by dividing the needle volume by flow rate. Volume fraction of the cell suspensions was calculated to be $<0.3\%$, thereby dilute enough to conform to Poiseuille flow relationships. Reynolds number was also calculated to determine flow conditions:

$$Re = \frac{\rho Q}{15\pi D\eta} \quad (2)$$

where ρ is density of PBS (treated as water at room temperature at $999.97 \text{ kg}/\text{m}^3$), Q is volumetric flow rate (ml/minute), D is the needle diameter, and η is the dynamic viscosity of the medium (0.001 Pas). For the lowest flow rate (10 $\mu\text{l}/\text{minute}$), Re is 1.33; for the highest flow rate (300 $\mu\text{l}/\text{minute}$), Re is 39.98 for 30G needles and 124.6 for 34G needles. These values are within the range for laminar flow ($Re < 2,000$).

To measure cell size, cells from each of the 3 batches used in this study were suspended to a concentration of 7×10^5 cells per milliliter and analyzed on a Coulter LS230 particle-size analyzer (Beckman Coulter, High Wycombe, U.K., <https://www.beckmancoulter.com>). Size distributions were obtained using the Fraunhofer approximation model, and size distribution plots based on volume distribution were generated.

Quantification of Cell Numbers Using the CyQUANT Assay

Cell suspensions (1.5×10^5 cells per milliliter) were ejected at various flow rates, as described, then transferred to clear 96-well plates (Costar; Corning Life Sciences, U.K., <https://www.corning.com>) and incubated for 24 hours. Cell number was then determined by quantification of total DNA by CyQUANT NF Cell Proliferation Assay (ThermoFisher Scientific, Paisley, U.K., <https://www.thermofisher.com>) according to manufacturer's instructions using a Tecan Infinite M200 microplate reader (Tecan, Reading, U.K., <http://www.tecan.com>), with excitation at 485 nm and emission detection at 535 nm. This method correlates DNA content (shown by fluorescence intensity) to the number of cells through the use of a reference standard curve, thereby providing an accurate measure of cell number.

CyQuant was also used to assess cell adhesion capacity 2 hours post-ejection, according to manufacturer's instructions. Briefly, well plates were prepared in duplicate and test well plates were washed gently with PBS to remove nonadherent cells. To determine total cell number, the directly plated control plate was centrifuged and culture medium was carefully removed. CyQuant working solution (100 μl) was added to each well. Plates were then incubated in the dark at 37°C for 1 hour. Adhesion capacity is expressed as fold difference relative to total cell number in the control plate.

Assessing Cell Recovery and Proliferation Using PrestoBlue

PrestoBlue (ThermoFisher Scientific) was used to determine 24-hour viability following ejection of cell suspensions (7×10^5 cells per milliliter), as well as proliferation over several days. A mixture of PrestoBlue and culture medium (1:9) was added to each well, and incubated in the dark at 37°C for 1 hour. Triplicate 100- μl aliquots were measured for fluorescence on a Tecan Infinite M200 microplate reader, using excitation and emission wavelengths of 560 and 590 nm, respectively.

Evaluating Cell Viability Using Live/Dead Viability/Cytotoxicity Assay

Assessment of viability was carried out according to manufacturer's instructions. Calcein AM and ethidium homodimer-1 were prepared in PBS to produce Live/Dead staining solution (ThermoFisher Scientific). Samples were visualized using a Nikon Eclipse TS100 microscope (Nikon, Kingston Upon Thames, U.K., <http://www.europe-nikon.com>). For flow cytometric analyses, samples were incubated with Live/Dead Viability/Cytotoxicity (ThermoFisher Scientific) staining solution for 30 minutes before analysis.

Apoptosis Assessment Using Annexin V/PI Analysis

Cells were analyzed using Alexa Fluor 488 Annexin V/Dead Cell Apoptosis Kit (ThermoFisher Scientific). Cells treated with 10 μM staurosporine (STS) were used as positive control. Briefly, cells were detached using Accutase Cell Dissociation Reagent (Cell Technologies, San Diego, CA, <http://www.accutase.com>) 24 hours post-ejection, washed with PBS, and centrifuged at $380g$ for 5 minutes. Cells were then resuspended in Annexin V-binding buffer, and 5 μl of Annexin V-FITC was added and incubated for 5 minutes. Next, 2 μl of propidium iodide was added and then incubated for a further 15 minutes. Annexin-binding buffer was then added, and cells were kept on ice in the dark until flow cytometric analysis.

Flow Cytometry Analysis

For flow cytometric analyses, a Beckman Coulter Cytomics FC500 flow cytometer (High Wycombe, U.K., <https://www.beckmancoulter.com>) using a 488-nm laser was used. Forward and side scatter data were also obtained and cross-referenced with fluorescence data. A sorting parameter of 10,000 total events was used, or 600 seconds per sample. Gating was performed using forward versus side scatter signals acquired on a linear scale, to exclude debris and clumps. Quadrants were determined using single stain and unstained control samples. Flow cytometry data were analyzed using WEASEL software (F. Batty, Walter and Eliza Hall Institute, Melbourne, Australia).

Apo-Tox Glo Triplex Assay

Cytotoxicity and apoptosis were assessed using ApoTox-Glo Triplex Assay (Promega, U.K., <https://www.promega.com>) according to the manufacturer's protocol, after ejecting cell suspensions (1.5×10^5 cells per milliliter) through 30G needles and then transferring them to clear 96-well plates (Corning Life Sciences). Fluorescence and luminescence readings were measured using a Tecan plate reader. To normalize well-to-well variability, cytotoxicity and caspase level measurements were represented as normalized to viability measurements (dead/live cell ratio and apoptotic/live cell

Table 1. Shear stress values and transit times through a 100- μ l Hamilton syringe attached to 30G and 34G 20-mm needles at the investigated flow rates^a

Flow rate (μ l/minute)	Shear stress in 30G needle (dyn/cm ²)	Shear stress in 34G needle (dyn/cm ²)	Transit time through syringe, seconds	Transit time through needle lumen, seconds
10	4.24	128.0	600	2.38
20	8.48	256.0	300	1.19
50	21.20	639.9	120	0.48
150	63.59	1,919.7	40	0.158
300	127.18	3,839.4	20	0.079

^aCalculated using Equation 1 in the text.

ratio). Cells exposed to 3 hours of 10 μ M STS treatment were used to provide a positive control.

Senescence Assay

We ejected 70 μ l of cell suspensions (7×10^5 cells per milliliter) at various flow rates, then transferred them to T-25 tissue culture flasks and incubated them for 3 days. Cells were tested using SA- β -galactosidase histochemical staining kit (Sigma-Aldrich, Dorset, U.K., <http://www.sigmaaldrich.com>) according to manufacturer's instructions. Senescence-associated β -galactosidase (SA- β -Gal) activity was determined by counting the number of blue-stained cells, determining an average percentage of number of stained cells to total cells. For each flow rate, at least 200 cells were counted from a minimum of 10 nonoverlapping microscopic fields in each flask.

Immunophenotyping

After ejection of the cell suspensions (7×10^5 cells per milliliter) at the various flow rates, cells were incubated overnight ($n = 3$). After 24 hours, flow cytometry-based immunophenotyping was carried out. Immunophenotypic analysis was carried out using a BD Stemflow hMSCs analysis kit and BD LSR II flow cytometer (BD Biosciences, London, U.K., <http://www.bdbiosciences.com>). Cells were prepared following manufacturer's instructions. Mouse anti-human monoclonal antibodies CD90 FITC, CD73 APC, and CD105 PerCP-Cy5.5 were used for positive identification of hMSCs; CD19, CD11b, CD34, CD45, and HLA-DR PE were used for negative expression. Isotype controls were prepared for all antibodies, and 10,000 events were recorded per sample.

Multilineage Differentiation Potential of Ejected MSCs

Cells were ejected through 30G needles at the various flow rates under investigation and tested for their ability to differentiate into adipogenic, osteogenic, and chondrogenic lineages. Uninduced controls were maintained in basal medium MSCGM (#PT-3001; Lonza).

Adipogenic Differentiation

Ejected hMSCs were seeded into 12-well plates for adipogenic differentiation. Cells were cultivated in MSCGM until confluence, then differentiation was induced with commercial adipogenic induction medium. The medium was altered between adipogenic induction and adipogenic maintenance media (#PT-3004; Lonza) for 3 days each time, per manufacturer's instructions. After 21 days, cultures were rinsed with 70% (volume per volume) isopropanol and differentiation was assessed by specific staining of lipid

droplets with 0.5% Oil Red O solution (Sigma-Aldrich, Poole, U.K., <http://www.sigmaaldrich.com>).

Osteogenic Differentiation

Ejected cell suspensions (1.5×10^5 cells per milliliter) were seeded in 12-well plates and cultured in osteogenic differentiation medium (#PT-3002; Lonza), which was changed every 3 days. After 21 days of incubation, cells were fixed in 10% (vol/vol) formalin and the presence of extracellular calcium deposits in wells containing differentiated cells was verified using Alizarin Red staining solution and von Kossa silver staining kit (Millipore, Feltham, Middlesex, U.K., <http://www.merckmillipore.com>). For Alizarin Red staining, cells were treated with Alizarin Red for 5 minutes at room temperature. After being washed three times in deionized water, cells were observed under a microscope. For von Kossa staining, cells were incubated with silver nitrate solution under exposure to ultraviolet (UV) light for 20 minutes. Wells were then washed with deionized water 3 times and treated with sodium thiosulfate solution for 5 minutes. Wells were then washed again three times with deionized water. Mineralized nodules were visualized as black spots.

Chondrogenic Differentiation

Micromass cultures were used for chondrogenic differentiation. Ejected cell suspensions were seeded in 20- μ l chondrogenic induction medium (#PT-3003; Lonza) in 96-well plates (Corning Life Sciences). After 2 hours, 200 μ l of chondrogenic induction medium was added to adherent cells, and medium was changed twice weekly. After 21 days, fixed cells were stained in 1% (weight per volume) Alcian blue solution (pH 1.5) overnight to identify the proteoglycan extracellular matrix. Nuclear fast red (Sigma #N3020; Sigma-Aldrich) counterstain was incubated for 5 minutes.

Investigation of Cell Retention in the Delivery Device

To investigate whether cells were preferentially retained in the syringe or needle, the syringe barrel and needle were separated following cell ejection at 10 μ l/minute, and each was then reattached to a corresponding clean syringe or needle. These were then flushed with PBS three times to dislodge retained cells, and washes were assessed for viable cells using PrestoBlue. To visualize cells retained in the delivery device, a Nikon SMZ1500 dissection microscope and a Zeiss LSM 510 UV META Kombi confocal system on an Axiovert 100 stand (Carl Zeiss, Jena, Germany, <http://www.zeiss.com>) were used.

To investigate the possible extent of adhesion to the delivery device, 100 μ l of cell suspensions with different densities (7×10^5 and 1.5×10^5 cells per milliliter) were seeded into 96-well glass-bottom

plates (Greiner Bio-One, Gloucester, U.K., <http://www.greinerbioone.com>) and incubated for 10 minutes at room temperature. Suspensions were then removed from the test wells using a pipette and left in the control wells. Some test wells were then gently washed three times with PBS to remove weakly adherent cells, and others were not washed and hence designated as “no-wash” wells. Control, no-wash, and washed wells were incubated for a further 4 hours to allow cell attachment, and cell numbers were quantified using the CyQuant assay. Fluorescence intensities of triplicate samples were normalized to control.

To assess whether the morphological changes of apoptosis, such as cellular shrinkage and membrane blebbing, may have led to a loss of cell-cell adhesion, we investigated ejected cell-dose recovery of apoptotic cells at 10 $\mu\text{l}/\text{minute}$ versus viable cells. Apoptosis was induced in hMSCs using 10 μM of staurosporine. Cell numbers ejected were then determined using CyQUANT NF Cell Proliferation Assay, as previously described.

Statistical Analysis

Statistical analyses were performed using GraphPad Prism 6 software (GraphPad Software, San Diego, CA, <http://www.graphpad.com>). Experiments were conducted with five needles for each batch of hMSCs tested, unless stated otherwise. Data sets were tested for normality and suitable tests of comparisons were subsequently chosen. Data were analyzed by one-way or two-way analysis of variance (ANOVA) with Dunnett’s post hoc test, unless otherwise stated. A p value $\leq .05$ was considered to be significant; mean values are given plus or minus the SD, unless otherwise indicated.

RESULTS

Cells from the 3 different donors, measured in triplicate, had a mean size of $22.57 \pm 1.34 \mu\text{m}$ and median size of $21.29 \pm 1.02 \mu\text{m}$ (supplemental online Fig. 1). The range of shear stress values generated in this investigation is presented in Table 1. Calculated shear stress values for 10 and 20 $\mu\text{l}/\text{minute}$ in 30G needles are in the range expected physiologically in the human circulation: Average wall shear stress is 1–6 dyn/cm^2 for venous circulation, and 15 dyn/cm^2 for arterial circulation [37, 38].

Effect of Varying Ejection Rates on Viability and Percentage Recovery of Dose Delivered

Figure 1A shows mean cell numbers quantified 24 hours after ejection of cell suspensions (prepared from 3 individual donors) through 30G needles, measured using the CyQuant assay. Percentage of dose delivered was significantly lower than the control value of directly pipetted cells at all flow rates tested ($p \leq .01$). In all donors tested, cells ejected at 300 $\mu\text{l}/\text{minute}$ showed the highest percentage cell dose delivered at $77.6\% \pm 11.7\%$. PrestoBlue was used to measure percentage of the dose delivered as viable cells 24 hours postejecction to confirm our findings (Fig. 1B). The proliferative ability of hMSCs at day 10 was not significantly affected following ejection (Fig. 1C).

All ejected cells attached to culture surfaces within 3 hours of ejection and displayed typical fibroblast-like morphology. The Live/Dead staining kit, which relies on esterase activity of living cells (green fluorescence) and compromised membranes of dead cells (red fluorescence), was used to assess viability within cells ejected. The proportion of viable cells was high among the flow rates tested (Figs 1D, 1E). However, a visibly lower number of cells appeared in ejected samples, particularly at 10 $\mu\text{l}/\text{minute}$,

suggesting cell loss during ejection and endorsing the results acquired using CyQuant and PrestoBlue assays. Figure 1E presents the flow cytometric analysis, which revealed a viability of $>97\%$ at all flow rates under investigation.

Effects of Varying Ejection Rates on Various Markers of Cellular Health

Multiplex assays are capable of measuring cell cytotoxicity, viability, and apoptosis simultaneously in a single well. To overcome well-to-well variations in cell numbers ejected with different ejection rates, the ApoTox-Glo Triplex Assay was used to measure cytotoxicity and apoptosis, and measurements were normalized to viability within the same well. There were statistically significant increases in cytotoxicity and caspase-3/7 activity levels in both donor samples ejected at 10 $\mu\text{l}/\text{minute}$ through 30G needles, compared with the directly pipetted control 4 hours postejecction (Fig. 2A).

Apoptosis was also assessed using Annexin V/PI: Annexin V⁻/PI⁻ cells were considered viable; Annexin V⁺/PI⁻, early apoptotic; Annexin V⁺/PI⁺, late apoptotic; and Annexin V⁻/PI⁺ were considered necrotic. After 24 hours, differences between samples were evident at the slower ejection rates used (Fig. 2B). The proportion of apoptotic cells was significantly higher in the samples ejected at slower flow rates, with $7.12\% \pm 2.2\%$ early apoptotic cells at 10 $\mu\text{l}/\text{minute}$ versus $4.93\% \pm 1.1\%$ in control samples. A trend of increasing necrotic cell proportions with increased ejection rates was also observed. The results indicate that loss of hMSC viability may still arise 24 hours postinjection, with increase in apoptotic cell populations in the ejected samples from the control being statistically significant at lower ejection rates.

SA- β -Gal was used to investigate whether cells undergo senescence because of the injection process. Supplemental online Figure 2A shows the quantification of stained SA- β -gal-positive cells observed after ejection, with a trend toward increased senescence with increasing ejection rates in cells derived from two donors. However, this increase was not statistically significant.

To assess the influence of ejection rate on the adhesion capacity of hMSCs, the numbers of adherent cells were determined by the CyQUANT NF Cell Proliferation Assay Kit 120 minutes postejecction, after gently washing twice with PBS. Adherent cell density was stated as fold difference relative to the control plate. Cell adhesion in test samples was not significantly different from that of control samples (supplemental online Fig. 2B).

Immunophenotyping

Following observations of apoptosis and senescence, we then attempted to determine whether ejection rate could also cause changes in expression of cell surface markers 24 hours after ejection. Flow cytometry-based immunophenotyping was carried out to measure surface markers as recommended by the International Society of Cellular Therapy (ISCT) [38]. Analysis showed that mesenchymal surface markers CD73, CD90, and CD105 were highly expressed ($>95\%$) in all control samples, whereas the markers CD11b, CD19, CD45, HLA-DR, and CD34 were negative ($<1\%$). Ejection of hMSCs at 10 $\mu\text{l}/\text{minute}$ caused a reduction of expression of all surface markers relative to the control (Table 2). There was a statistically significant downregulation of expression of CD105 in both donor samples ($93.2\% \pm 0.6\%$ and $93.5\% \pm 1.2\%$) at the slowest flow rates under investigation ($p \leq .05$) in comparison with controls.

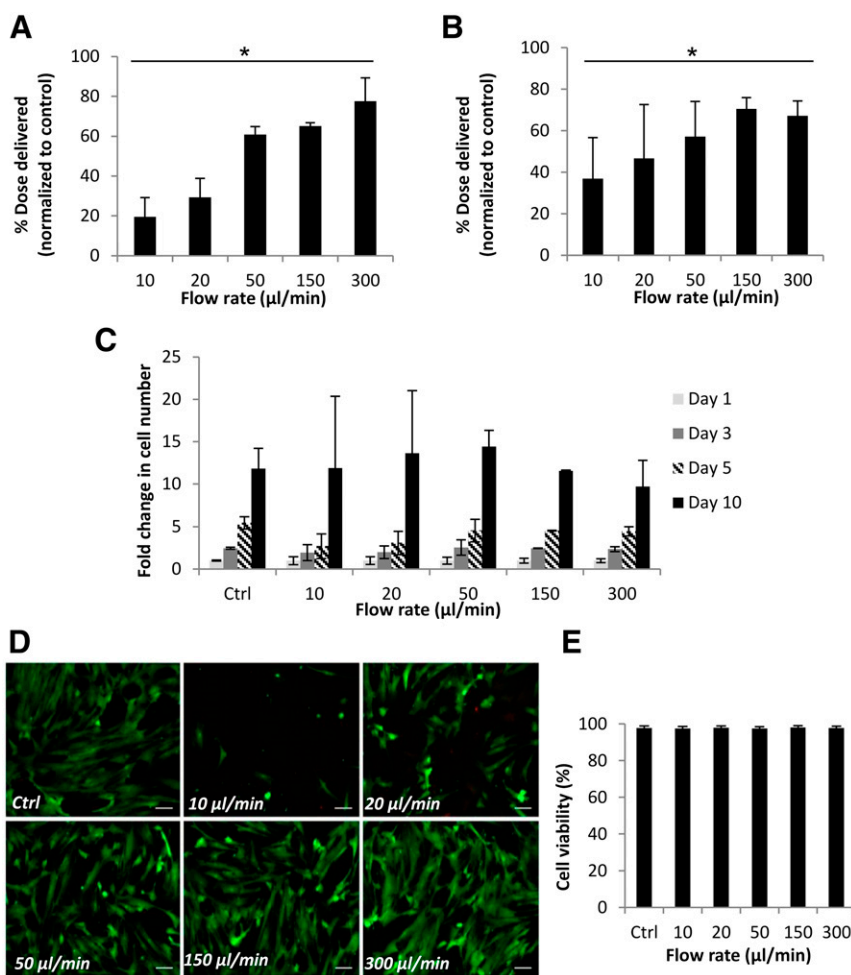


Figure 1. Viability of human mesenchymal stem cells (hMSCs) and percentage of cell dose delivered via 30G needles. **(A):** Percentage of hMSCs delivered, determined using CyQuant, following ejection through a 30G 20-mm needle. Data were normalized against a control value of directly plated cells. Data represent averages from 3 donors ($n = 5$ each) in 5 independent experiments (mean \pm SD). *, $p \leq .01$ for number of ejected cells compared with control (one-way analysis of variance [ANOVA] with Dunnett’s post hoc test). **(B):** Percentage of hMSCs delivered as viable cells, measured using PrestoBlue, following ejection via a 30G needle (mean \pm SD). Data are combined from 3 independent donors and 3 independent experiments ($n = 3$ each), each measured in triplicate. *, $p \leq .05$ for number of viable ejected cells and control sample (one-way ANOVA with Dunnett’s post hoc test). **(C):** Representative graph showing proliferation of hMSCs (because of variants in proliferation rate between donors), given as fold change in number from day 0 of each sample, measured using PrestoBlue (mean \pm SD; $n = 3$; measured in triplicate). **(D):** Representative Live/Dead-stained fluorescence images of hMSCs 48 hours following ejection at various flow rates. Scale bar = 50 μ m. **(E):** Graph shows flow cytometric analysis of ejected hMSCs (three independent experiments), illustrating high viable cell proportions at all flow rates under investigation. Abbreviation: Ctrl, control.

Effects of Varying Needle Gauge

Smaller needles are essential clinically for high-accuracy applications to reduce physical damage, especially for retinal or neural regenerative applications. To explore cell viability and recovery following ejection through smaller needle sizes, hMSCs were injected through 34G 20-mm needles at all the flow rates under investigation. Cells ejected through both 30G and 34G 20-mm needles exhibited the same trend of percentage cell recovery with flow rates tested, with cells ejected via 34G needles at 300 μ l/minute displaying the greatest cell recovery (64.4% \pm 16.3%). However, the use of 34G needles resulted in a larger reduction in the percentage of cell dose delivered compared with the 30G needle at all rates under investigation (Fig. 3A). Microscopic examination of ejected cells stained with Live/Dead staining solution exhibited a high percentage of cells positive for calcein AM (Fig. 3B).

Figure 3C shows the apoptotic and necrotic cell fractions in cell samples from three donors; the samples were ejected via 34G needles, across all flow rates after 24 hours of incubation. A trend toward increased apoptosis was observed with this smaller needle diameter. Additionally, a significant increase in early apoptotic cell proportions was observed with the highest flow rate under investigation as well as the slowest flow rate ($p < .05$), unlike the results previously observed with the larger needle gauge (Fig. 2B). Table 1 illustrates that shear forces exerted on the cells ejected through 34G needles at the lowest flow rate under investigation are higher than those calculated for all flow rates with a 30G needle. This suggests that there may be an optimum flow rate that balances the exerted mechanical forces with the time spent exposed to these forces. The high variability of apoptotic cell proportions in the case of 34G needles is possibly attributable to uneven injection flow, due to its extremely small diameter (51 μ m).

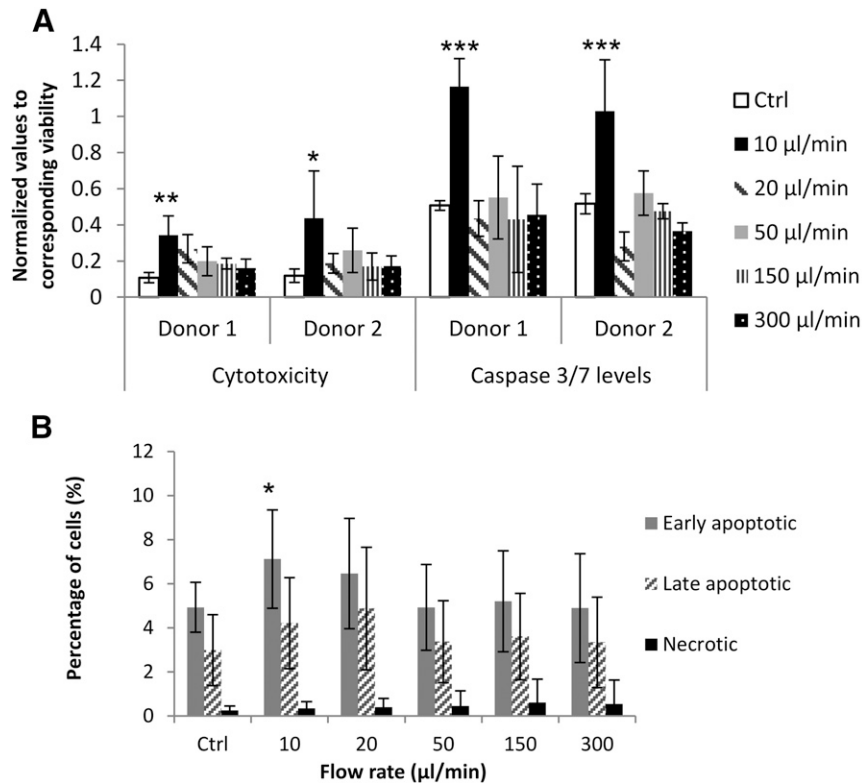


Figure 2. Cytotoxicity and apoptosis levels of human mesenchymal stem cells (hMSCs) ejected via 30G needles. **(A):** Cytotoxicity and apoptosis measurements in hMSCs from 2 donors 4 hours postejction (analyzed by ApoTox-Glo Triplex Assay). Cytotoxicity and caspase-3/7 activity measurements were normalized to viability within the same well. 10 μM staurosporine treatment was used as positive control ($n = 5$; mean \pm SD). *, $p \leq .05$; **, $p < .01$; ***, $p < .0001$. **(B):** Percentages of apoptotic and necrotic cells 24 hours postinjection, measured using Alexa Fluor 488 Annexin V/PI (3 donors in 6 independent experiments; $n = 15$). *, $p \leq .05$ for comparison of samples and control using analysis of variance with Dunnett's post hoc test. Abbreviation: Ctrl, control.

Table 2. Immunophenotypic characteristics of human mesenchymal stem cells in control and samples ejected through 30G needles by multicolor flow cytometry 24 hours postejction

Marker	Average % of positive cells \pm SD ^a					
	Control	10 μl/minute	20 μl/minute	50 μl/minute	150 μl/minute	300 μl/minute
CD90	99.3 \pm 0.45	98.5 \pm 1.26	99.3 \pm 0.44	99.6 \pm 0.15	99.5 \pm 0.35	99.5 \pm 0.18
CD105	95.4 \pm 0.50	93.3 \pm 0.85 ^b	94.3 \pm 2.18	96.1 \pm 0.76	95.8 \pm 0.98	95.7 \pm 1.25
CD73	99.0 \pm 0.73	97.9 \pm 1.73	98.9 \pm 0.61	99.2 \pm 0.45	99.2 \pm 0.55	99.2 \pm 0.33
Negative markers	0.21 \pm 0.24	0.18 \pm 0.13	0.98 \pm 2.0	0.15 \pm 0.11	0.11 \pm 0.093	0.15 \pm 0.17

^a $n = 6$ using cells from 2 independent donors.

^b $p \leq .05$, one-way analysis of variance followed by Dunnett's post hoc test.

Trilineage Differentiation Potential of Ejected hMSCs

The ability of hMSCs to differentiate into multiple lineages is a functional criterion defining them [38]. Figure 4 is representative of results obtained with cells from at least 2 donors ($n = 5$ each), and shows that all control and ejected samples completed multilineage differentiation. After 21 days of induction toward an adipogenic lineage, a distinctive morphological change with appearance of lipid vacuoles was observed. Osteogenesis was assessed by staining for calcium and phosphate after 21 days of culture under osteogenic conditions, with all samples exhibiting positive staining with Alizarin Red and von Kossa stains. Additionally, all cells retained chondrogenic differentiation capacity, as shown by positive staining using Alcian blue. All hMSCs showed similar differentiation patterns. However, there was an observable difference in both the number

of cells at day 21 and the extent of both adipogenic and osteogenic differentiation in the samples ejected at 10 μl/minute.

Investigating Low Cell Recovery at Slow Ejection Rates

Additional investigations were undertaken to explore potential reasons behind the smaller cell numbers ejected at lower ejection rates. Each ejection was followed by PBS washes ($5 \times 100 \mu\text{l}$) at 300 μl/minute to dislodge cells that may have transiently adhered to the inner surfaces of the syringe or needle. Washes were combined, and cell numbers measured using PrestoBlue. Figure 5A shows cell numbers of the directly plated controls, ejected samples, and those quantified in the succeeding PBS washes. A trend can be clearly detected where the number of viable cells in the PBS washes was increased at lower flow rates, signifying that

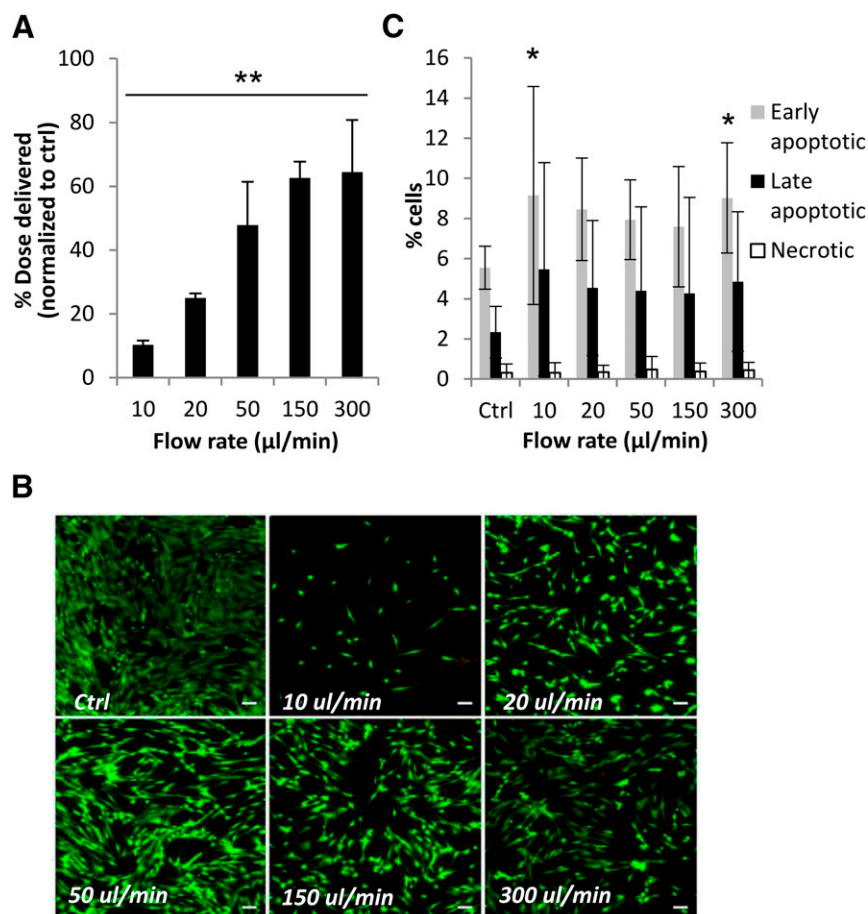


Figure 3. Viability and apoptosis levels of human mesenchymal stem cells (hMSCs) delivered via 34G needles. **(A):** Percentage of hMSCs delivered 24 hours postinjection via 34G 20-mm needles. Results are normalized mean values to control \pm SD (averages from 2 donors and 2 independent experiments, each $n = 5$). **, $p \leq .01$ one-way analysis of variance (ANOVA). **(B):** Representative fluorescence images depicting Live/Dead-stained hMSCs ejected at several flow rates 48 hours postinjection. Scale bar = 100 μ m. **(C):** Mean percentages (\pm SD) of apoptotic and necrotic cells 24 hours postinjection via 34G needles, measured using Alexa Fluor 488 Annexin V/PI (3 donors in 5 independent experiments; $n = 11$). *, $p \leq .05$ for comparison of samples and control (ANOVA and Dunnett's post hoc test). Abbreviation: Ctrl, control.

the adhesive nature of hMSCs may have caused them to adhere to the delivery device at the lower flow rates. Cells also were observed visibly aggregating in the syringe barrel as the plunger advanced during PBS washes postinjection at the slowest flow rates (Fig. 5B), and were visualized in the syringe postinjection before PBS washes (Fig. 5C).

To explore whether cells were preferentially retained in the syringe or needle, components of the delivery device (syringe barrel and needle) were separated following ejection of cell suspensions at 10 μ l/minute, and each was then reattached to a corresponding clean syringe or needle. These were then flushed with 100 μ l of PBS 3 times to dislodge any retained cells, and washes were assessed for viable cells, using PrestoBlue. Most of the cells were retained in the syringe (21.5% \pm 9.5%) relative to 5.6% \pm 6.4% retained in the needle (Fig. 5D).

To investigate whether 10 minutes in the delivery device (for 10 μ l/minute samples) would account for the loss in cell dose delivered, cells suspensions with different densities (7×10^5 and 1.5×10^5 cells per milliliter) were seeded into well-plates with glass bottoms (made of borosilicate glass to simulate the Hamilton syringe) and incubated for 10 minutes at room temperature. A comparison was then made between wells from which the cell suspensions were removed and those that underwent gentle washes

of PBS after removal of cell suspensions. Fluorescence readings were normalized to control wells.

After 10 minutes of incubation, almost 55% of the cell population adhered to the surface following removal of the suspension from the wells. Gentle washes resulted in 26.9% of cells still being retained in the wells with high-density suspensions, and 10.7% of cells being retained in the low-density suspensions under investigation (Fig. 5E).

Apoptosis was induced in hMSCs using 10 μ M staurosporine, which was shown by Annexin V/PI staining to result in an apoptotic population of 89.95% \pm 2.14% ($n = 4$) in comparison with 7.58% \pm 1.85% ($n = 4$) apoptotic cells in normal, viable populations. A comparison of cell-dose delivery between apoptotic and viable cells at 10 μ l/minute was carried out ($n = 4$) using cells from 2 different donors. At an ejection rate of 10 μ l/minute, 8.89% \pm 1.99% of the viable cell dose was ejected, in comparison with 28.8% (SEM, \pm 7.65%) of the apoptotic cell dose ejected at the same rate (Mann-Whitney test, $p < .05$) (Fig. 5F).

DISCUSSION

This study emphasizes the importance of optimization of injection parameters as a critical aspect of designing and comparing

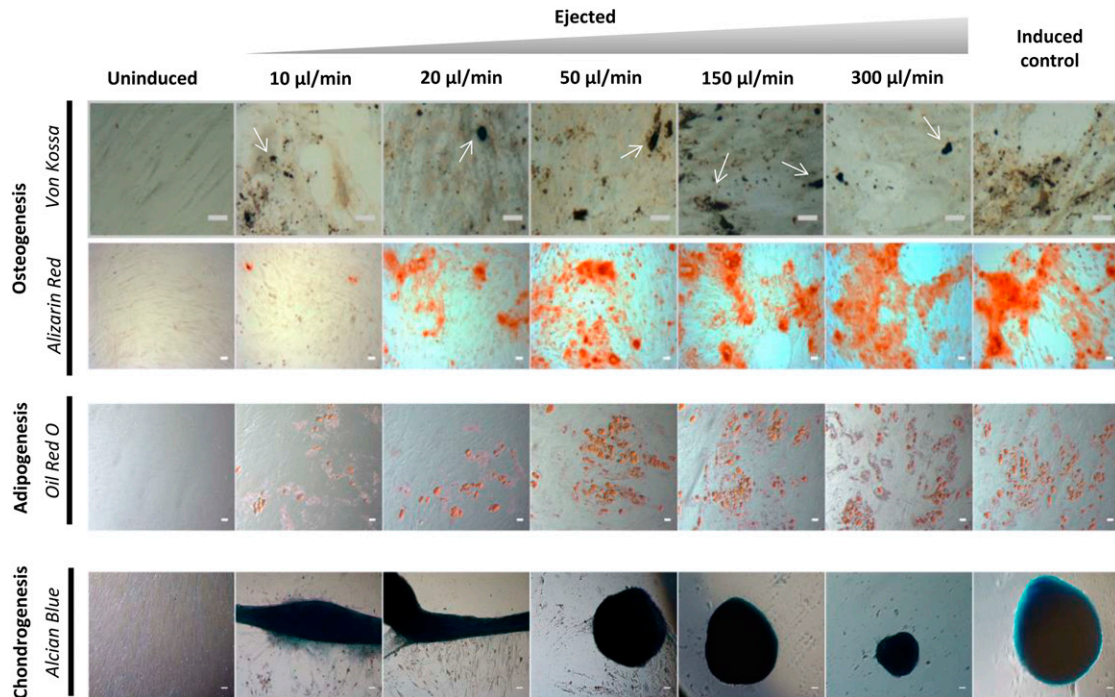


Figure 4. Trilineage differentiation potential of cultured human mesenchymal stem cells (hMSCs) ejected via 30G needles. To verify the differentiation capacity of ejected hMSCs via 30G needles, adipogenic, osteogenic, and chondrogenic differentiation was carried out on ejected and control samples following 21 days of differentiation. Adipogenic differentiation was assessed by Oil Red O staining. Osteogenic differentiation was assessed by Alizarin Red staining of calcified matrix. Phase-contrast microscopy of micromass cultures shows differentiation down the chondrocyte lineage, as confirmed by Alcian Blue staining. In Von Kossa-stained samples, calcified deposits are indicated by white arrows. Scale bar = 50 μm . Cells cultured in mesenchymal stem cell growth medium without induction served as a negative control.

clinical studies using cell transplantation. The aim of this study was to examine the impact of administration of hMSCs via a syringe-based delivery system on cellular health, which is vital to their survival postejction. With the increase in number of cell-therapy clinical trials and variability of results obtained, there is an urgent need to step back and evaluate key factors required for the optimal delivery of viable cells.

Limited studies are currently available that assess clinically relevant cell types, needles, and ejection rates. hMSCs used in this study were found to have a mean size of 22.57 μm , making them comparatively large relative to needle gauges appropriate for high-accuracy cell-therapy applications. All donors used were within a small age range (supplemental online Table 1), and there were no discernible differences in cell-health parameters pre- or postejction between male and female donors used in this study.

Ejection rates used in clinical trials were found to be highly variable: For neural cell transplantation, for example, a rate of 5 $\mu\text{l}/\text{minute}$ has been used [40]; 300 $\mu\text{l}/\text{minute}$ has been used for spinal injury [41]; and several ejection rates ranging between 10 and 1000 $\mu\text{l}/\text{minute}$ have been used for stroke [42, 43]. Therefore, ejection rates used in this study (10–300 $\mu\text{l}/\text{minute}$) were selected to assess a range of clinically relevant ejection rates previously used in clinical trials. Calculated values for shear stress (Table 1) at 10 and 20 $\mu\text{l}/\text{minute}$ in 30G needles were in the range expected in human circulation. All other flow rates had shear stress values outside the ranges for venous and arterial circulations [37, 38]. Most of the shear stress values calculated suggest that cells are being exposed to supraphysiological mechanical stresses during the injection process, and, therefore, it is deemed

critical to assess the effects of such stresses on cellular health. The impact of injectable delivery on hMSCs was quantified in terms of 24-hour viability, apoptosis, and other aspects of cell health.

PrestoBlue and CyQUANT assays were used to measure viability in terms of cell numbers obtained relative to directly pipetted control samples. A significant loss of cells at all flow rates under investigation was observed at 24 hours postejction. The percentage of hMSCs delivered was directly proportional to the ejection rate used, with cells ejected at 300 $\mu\text{l}/\text{minute}$ displaying the highest percentage of cells delivered. This may be due to the shorter time spent subjected to mechanical forces within the delivery device at this flow rate, which appears to have a more prominent effect on the cells than the size of shear stress exerted at the rates under investigation. This is interesting to compare with the smaller NIH 3T3 cells used in our previous study [32] (mean size, 14.9 μm), which, unlike hMSCs, had an optimum cell-dose delivery at 150 $\mu\text{l}/\text{minute}$, after which delivery efficiency decreased. Percentages of cell recovery at slower ejection rates were confirmed microscopically, where lower flow rates resulted in the ejection of a visibly lower number of cells. Flow cytometric analyses measured proportions of dead cells delivered through the needle within samples under investigation. Live/Dead analyses (Fig. 1D, 1E) confirmed that cells obtained by ejection through 30G needles at all flow rates were not discernibly affected (viable cells >97%). This is comparable with previous viability findings with various cell types, where viability was >90% at the needle sizes investigated in those studies [16, 18, 19]. Because cell viability was high at all flow rates investigated, it was concluded that cell loss probably was mainly due to retention in the delivery device.

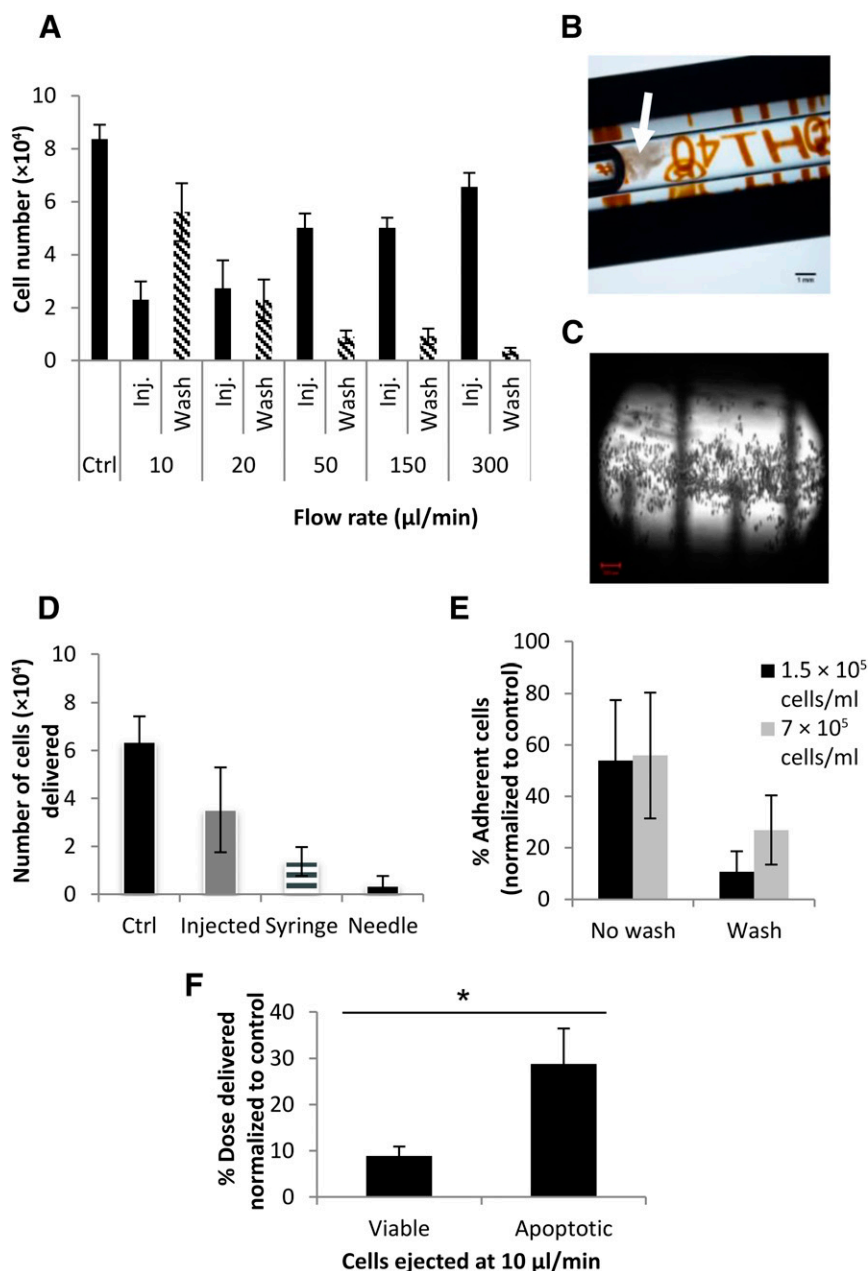


Figure 5. Investigation of cell recovery and retention in the delivery device following ejection via 30G needles. **(A):** To investigate poor cell recovery at slow flow rates, each ejection was followed by phosphate-buffered saline (PBS) washes ($5 \times 100 \mu\text{l}$ at $300 \mu\text{l}/\text{minute}$), and the number of cells recovered was quantified using PrestoBlue (mean \pm SEM; 2 donors; each $n = 3$). **(B):** A representative dissection microscope image of a syringe barrel postejection at $10 \mu\text{l}/\text{minute}$, depicting cells that have been retained in the syringe aggregating during PBS wash. Scale bar = 1 mm. **(C):** Confocal microscopy was used to image cells retained in the syringe postejection at $10 \mu\text{l}/\text{minute}$. Scale bar = $200 \mu\text{m}$. **(D):** To investigate where cells were being retained in the delivery device, its components (syringe barrel and needle) were separated after ejection at $10 \mu\text{l}/\text{minute}$, and each was separately washed with PBS. The number of cells recovered was measured using PrestoBlue (mean \pm SEM; $n = 3$). **(E):** Adhesion of cells to a borosilicate glass surface was assessed, comparing the number of cells adhering with no wash following removal of cell suspensions from wells and after gentle PBS washes ($100 \mu\text{l}$; $n = 3$; 3 independent experiments using cells from 3 donors). **(F):** A comparison of cell-dose recovery between viable and apoptotic cells (induced using $10 \mu\text{M}$ staurosporine) ejected at $10 \mu\text{l}/\text{minute}$ ($n = 4$). *, $p \leq .05$ for the difference between the 2 groups, using the Mann-Whitney test. Abbreviations: Ctrl, control; Inj., injected.

Cell viability assays are a valuable key indicator of potential damage to cells. However, the cells' transient exposure to supra-physiological shear-stress forces (Table 1) may trigger apoptotic responses and other changes at the molecular level. Therefore, further investigation into the apoptotic, senescence, and phenotypic expressions of the ejected hMSCs was carried out. The

proliferative capacity of the cells ejected through 30G needles did not show any significant changes with all flow rates under investigation. However, a significant increase in caspase-3/7 protein levels occurred as early as 4 hours postejection. Multiplexing viability, cytotoxicity, and apoptosis assays in the same culture well provided us with internal controls to determine

caspase-3/7 levels while taking the differences in cell numbers ejected into account, in contrast with previous studies [17, 19]. This multiplex assay indicated that the slowest ejection rate under investigation (10 $\mu\text{l}/\text{minute}$) significantly increased cytotoxicity and apoptosis levels in ejected hMSCs. An increase in the apoptotic cell proportions at the slowest flow rates and an increase in the necrotic cell proportions were also observed at 24 hours post-ejection with Annexin V/PI staining. This suggests that slower flow rates prolonged cell exposure to shear forces, possibly inducing apoptosis. Since the lowest flow rates resulted in a significant increase in apoptotic cell proportions compared with the control, this endorsed the hypothesis that an equilibrium needs to be achieved between the mechanical forces exerted on the cells and the period of time spent subjected to these forces. The senescence results displayed a different trend, where SA- β -galactosidase activity increased with increasing flow rates, but this failed to reach significance.

The ICST defines MSCs as cells that are capable of osteogenesis, adipogenesis, and chondrogenesis under *in vitro* conditions, and that are positive (>95%) for CD73, CD90, and CD105 but negative for CD11b, CD14, CD34, CD45, CD79a, and HLA-DR surface markers [39]. Downregulation in expression of CD105, a stromal cell-associated marker, to less than 95% at 24 hours post-ejection at the slowest rate of ejection under investigation (10 $\mu\text{l}/\text{minute}$) represented the greatest significant change observed in flow cytometric immunophenotyping. This is lower than the value stated by ICST as minimal criteria to define hMSCs. Downregulated expression of CD105 has been observed after MSC differentiation and can be used to indicate their differentiation status [44]. Therefore, altered expression of this surface marker at the slowest flow rates investigated may affect the multipotency of hMSCs and, therefore, impact the therapeutic efficiency of the injected cells. The capacity to differentiate into the three lineages was subsequently investigated.

Targeted cell lineage differentiation is vital for the regenerative effect of MSCs. We investigated the capacity for multilineage differentiation of the ejected hMSCs. All samples completed multilineage differentiation, which was induced using the manufacturer's recommended protocols. The progression of differentiation, indicated via qualitative markers of adipogenesis, osteogenesis, and chondrogenesis, was consistent with previous studies in terms of retention of differentiation capacity [16, 17]. However, differentiation was visibly lower at the slower ejection rates, which was confirmed by standard staining methods. This may have been due to lower cell numbers being ejected at these rates, impairing the capacity for differentiation. Elucidation of the extent of impact of ejection rate on differentiation capacity cannot be concluded using qualitative staining methods alone, and this requires further more detailed investigation.

Needle gauge also had a substantial impact on viability post-ejection. A smaller percentage of the delivered cell dose was observed with the smaller needle diameter (51 μm). This can be explained by the magnitudes of the forces to which cells are exposed: Smaller needles will result in higher forces being exerted on the cells. In addition, higher flow rates also caused significantly higher apoptotic cell proportions, which may be due to the higher, supraphysiological shear-force levels exerted at this flow rate (Table 1). In the case of 34G needles, both the prolonged ejection period at 10 $\mu\text{l}/\text{minute}$ and higher shear-force value exerted at 300 $\mu\text{l}/\text{minute}$ adversely impacted cells post-ejection, causing significantly higher apoptotic cell proportions

than control samples. Flow rates in between these lower and upper limits seemed to maintain a more favorable balance for the ejected cells.

Since cytotoxicity and apoptosis results did not fully account for the substantial differences in percentages of cell doses delivered, the likelihood of cells adhering to the inner walls of the delivery device was investigated, because hMSCs are highly adherent anchorage-dependent cells [45]. Results revealed that cells were mainly retained in the syringe, and a smaller proportion was retained on the inner walls of the needle. These were only dislodged by PBS washes at 300 $\mu\text{l}/\text{minute}$. Cell loss occurring at the slower flow rates may be due to the longer period of time that the cells are in contact with the syringe glass surface, which may allow the formation of transient adhesions to the injector and other cells, forming aggregates. The present results demonstrate that such adhesive interactions with the delivery device can be significant and could substantially affect the delivery of cells to the target site. This highlights the importance of developing materials that do not promote the attachment of cells for the manufacture of cell-delivery devices. In addition, the optimization of injection rates used in preclinical and clinical trials is critical to reduce mechanical stress and improve cell-delivery success rates.

We also decided to investigate whether the characteristic morphological changes associated with apoptosis, such as cellular shrinkage and membrane blebbing [46], led to the increase in apoptotic cell proportions recovered at slower ejection rates, or whether it was due to the increased time exposed to mechanical forces within the delivery device. Percentage of cell-dose delivery between apoptotic cells (induced using 10 μM staurosporine) and viable cells ejected at 10 $\mu\text{l}/\text{minute}$ was compared. Despite the lower cell-adhesion capability exhibited by apoptotic cells, shown by the statistically significant increase in cell dose delivered (Mann-Whitney test, $p < .05$), the increase in percentage delivered was not substantial. This suggests that the increase in apoptosis levels at a slower flow rate results from a combination of both factors: the prolonged exposure to shear forces, as well as the lower capacity of apoptotic cells to form transient adhesions to the syringe.

CONCLUSION

MSCs have recently emerged as excellent candidates for cell therapy. Although great progress has been achieved, future research should focus on elucidating optimal strategies for injectable cell delivery, to revolutionize regenerative cellular therapies. Our results emphasize the importance of adapting cell-administration protocols to the nature of transplanted cells, because it is reasonable to assume that the environment into which the cells would be injected would also have further adverse effects on injected cells. Initial loss of injected cells may be due to a combination of cell disruption by mechanical forces and cell retention in the delivery device. Results of this study reveal that passing hMSCs through a needle at the slower flow rates used previously in various clinical trials is likely to induce apoptosis, which can bring about delayed death of the injected hMSCs, and phenotypic expression changes, which may impact their physiological functioning. In comparison with our previous study using NIH 3T3 cells, the percentage of viable hMSCs delivered increased with increasing ejection rate, whereas the smaller NIH 3T3 cells had an optimum ejection rate of 150 $\mu\text{l}/\text{minute}$, after which efficiency of delivery

dropped. Therefore, this study emphasizes the importance of thorough consideration of administration protocols required for efficacious cell delivery. Further studies will enable us to optimize protocols using finer needles to minimize the physical damage of cell implantation, particularly for degenerative diseases accompanying neuronal damage.

ACKNOWLEDGMENTS

We thank Dr. David Onion for assistance with flow cytometry, and Dr. Tim Self and Dr. Robert Markus for help with confocal microscopy. This work was supported by the U.K. Regenerative Medicine Platform Hub for Acellular Technologies. M.H.A. is funded by a University of Nottingham International Office scholarship, the Faculty

for the Future Program of the Schlumberger Foundation, and Misr El-Kheir Foundation.

AUTHOR CONTRIBUTIONS

M.H.A.: design, collection and assembly of data, data analysis and interpretation, manuscript writing; F.R.A.J.R. and L.J.W.: revision of manuscript, final approval of manuscript; K.M.S.: conception, financial support, revision of manuscript, final approval of manuscript.

DISCLOSURE OF POTENTIAL CONFLICTS OF INTEREST

The authors indicated no potential conflicts of interest.

REFERENCES

- Hare JM, Traverse JH, Henry TD et al. A randomized, double-blind, placebo-controlled, dose-escalation study of intravenous adult human mesenchymal stem cells (prochymal) after acute myocardial infarction. *J Am Coll Cardiol* 2009;54:2277–2286.
- Mendez I, Sanchez-Pernaute R, Cooper O et al. Cell type analysis of functional fetal dopamine cell suspension transplants in the striatum and substantia nigra of patients with Parkinson's disease. *Brain* 2005;128:1498–1510.
- Jiang LH, Yang NY, Yuan XL et al. Dacosterol promotes the proliferation of neural stem cells. *J Steroid Biochem Mol Biol* 2014;140:90–99.
- Le R, Kou Z, Jiang Y et al. Enhanced telomere rejuvenation in pluripotent cells reprogrammed via nuclear transfer relative to induced pluripotent stem cells. *Cell Stem Cell* 2014;14:27–39.
- Phinney DG, Prockop DJ. Concise review: Mesenchymal stem/multipotent stromal cells: The state of transdifferentiation and modes of tissue repair—current views. *STEM CELLS* 2007;25:2896–2902.
- Srijaya TC, Ramasamy TS, Kasim NH. Advancing stem cell therapy from bench to bedside: Lessons from drug therapies. *J Transl Med* 2014;12:243.
- Caplan AI. Why are MSCs therapeutic? New data: New insight. *J Pathol* 2009;217:318–324.
- Martens TP, See F, Schuster MD et al. Mesenchymal lineage precursor cells induce vascular network formation in ischemic myocardium. *Nat Clin Pract Cardiovasc Med* 2006;3(suppl 1):S18–S22.
- Karp JM, Leng Teo GS. Mesenchymal stem cell homing: The devil is in the details. *Cell Stem Cell* 2009;4:206–216.
- Miljan EA, Sinden JD. Stem cell treatment of ischemic brain injury. *Curr Opin Mol Ther* 2009;11:394–403.
- Teng CJ, Luo J, Chiu RC et al. Massive mechanical loss of microspheres with direct intramyocardial injection in the beating heart: Implications for cellular cardiomyoplasty. *J Thorac Cardiovasc Surg* 2006;132:628–632.
- Müller-Ehmsen J, Whittaker P, Kloner RA et al. Survival and development of neonatal rat cardiomyocytes transplanted into adult myocardium. *J Mol Cell Cardiol* 2002;34:107–116.
- Suzuki K, Murtuza B, Beauchamp JR et al. Role of interleukin-1beta in acute inflammation and graft death after cell transplantation to the heart. *Circulation* 2004;110(suppl 1):II219–II224.
- Bliss TM, Kelly S, Shah AK et al. Transplantation of hNT neurons into the ischemic cortex: Cell survival and effect on sensorimotor behavior. *J Neurosci Res* 2006;83:1004–1014.
- Aguado BA, Mulyasmita W, Su J et al. Improving viability of stem cells during syringe needle flow through the design of hydrogel cell carriers. *Tissue Eng Part A* 2012;18:806–815.
- Mamidi MK, Singh G, Husin JM et al. Impact of passing mesenchymal stem cells through smaller bore size needles for subsequent use in patients for clinical or cosmetic indications. *J Transl Med* 2012;10:229.
- Walker PA, Jimenez F, Gerber MH et al. Effect of needle diameter and flow rate on rat and human mesenchymal stromal cell characterization and viability. *Tissue Eng Part C Methods* 2010;16:989–997.
- Heng BC, Hsu SH, Cowan CM et al. Transcatheter injection-induced changes in human bone marrow-derived mesenchymal stem cells. *Cell Transplant* 2009;18:1111–1121.
- Agashi K, Chau DYS, Shakesheff KM. The effect of delivery via narrow-bore needles on mesenchymal cells. *Regen Med* 2009;4:49–64.
- Tol M, Akar AR, Durdu S et al. Comparison of different needle diameters and flow rates on bone marrow mononuclear stem cell viability: An ex vivo experimental study. *Cytotherapy* 2008;10:98–99.
- Chen X, Thibeault S. Effect of DMSO concentration, cell density and needle gauge on the viability of cryopreserved cells in three dimensional hyaluronan hydrogel. *Conf Proc IEEE Eng Med Biol Soc* 2013;2013:6228–6231.
- Kondziolka D, Gobbel GT, Fellows-Mayle W et al. Injection parameters affect cell viability and implant volumes in automated cell delivery for the brain. *Cell Transplant* 2011;20:1901–1906.
- Kondziolka D, Steinberg GK, Cullen SB et al. Evaluation of surgical techniques for neuronal cell transplantation used in patients with stroke. *Cell Transplant* 2004;13:749–754.
- Center for Biologics Evaluation and Research. Guidance for FDA reviewers and sponsors: Content and review of chemistry, manufacturing, and control (CMC) information for human somatic cell therapy investigational new drug applications (INDs). 2008. Available at <http://www.fda.gov/BiologicsBloodVaccines/Guidance-ComplianceRegulatoryInformation/Guidances/Xenotransplantation/ucm074131.htm>.
- Meluz n J, Mayer J, Groch L et al. Autologous transplantation of mononuclear bone marrow cells in patients with acute myocardial infarction: The effect of the dose of transplanted cells on myocardial function. *Am Heart J* 2006;152:975.e979–915.
- Quyyumi AA, Waller EK, Murrow J et al. CD34(+) cell infusion after ST elevation myocardial infarction is associated with improved perfusion and is dose dependent. *Am Heart J* 2011;161:98–105.
- Hare JM, Fishman JE, Gerstenblith G et al. Comparison of allogeneic vs autologous bone marrow-derived mesenchymal stem cells delivered by transcatheter injection in patients with ischemic cardiomyopathy: The POSEIDON randomized trial. *JAMA* 2012;308:2369–2379.
- Kebriaei P, Isola L, Bahceci E et al. Adult human mesenchymal stem cells added to corticosteroid therapy for the treatment of acute graft-versus-host disease. *Biol Blood Marrow Transplant* 2009;15:804–811.
- Shehadah A, Chen J, Pal A et al. Human placenta-derived adherent cell treatment of experimental stroke promotes functional recovery after stroke in young adult and older rats. *PLoS One* 2014;9:e86621.
- Borlongan CV, Weiss MD. Baby STEPS: A giant leap for cell therapy in neonatal brain injury. *Pediatr Res* 2011;70:3–9.
- Wei X, Yang X, Han ZP et al. Mesenchymal stem cells: A new trend for cell therapy. *Acta Pharmacol Sin* 2013;34:747–754.
- Amer MH, White LJ, Shakesheff KM. The effect of injection using narrow-bore needles on mammalian cells: Administration and formulation considerations for cell therapies. *J Pharm Pharmacol* 2015;67:640–650.
- Qiao LY, Huang FJ, Zhao M et al. A two-year follow-up study of cotransplantation with neural stem/progenitor cells and mesenchymal stromal cells in ischemic stroke patients. *Cell Transplant* 2014;23(suppl 1):S65–S72.
- Liu Q, Li RT, Qian HQ et al. Targeted delivery of miR-200c/DOC to inhibit cancer stem cells and cancer cells by the gelatinases-stimuli nanoparticles. *Biomaterials* 2013;34:7191–7203.
- Salama H, Zekri AR, Medhat E et al. Peripheral vein infusion of autologous mesenchymal stem cells in Egyptian HCV-positive patients with

end-stage liver disease. *Stem Cell Res Ther* 2014;5:70.

36 Jiang Y, Zhu W, Zhu J et al. Feasibility of delivering mesenchymal stem cells via catheter to the proximal end of the lesion artery in patients with stroke in the territory of the middle cerebral artery. *Cell Transplant* 2013;22:2291–2298.

37 Reneman RS, Hoeks AP. Wall shear stress as measured in vivo: Consequences for the design of the arterial system. *Med Biol Eng Comput* 2008;46:499–507.

38 Malek AM, Alper SL, Izumo S. Hemodynamic shear stress and its role in atherosclerosis. *JAMA* 1999;282:2035–2042.

39 Dominici M, Le Blanc K, Mueller I et al. Minimal criteria for defining multipotent mesenchymal stromal cells. The International Society for

Cellular Therapy position statement. *Cytotherapy* 2006;8:315–317.

40 Glass JD, Boulis NM, Johe K et al. Lumbar intraspinal injection of neural stem cells in patients with amyotrophic lateral sclerosis: Results of a phase I trial in 12 patients. *STEM CELLS* 2012;30:1144–1151.

41 Yoon SH, Shim YS, Park YH et al. Complete spinal cord injury treatment using autologous bone marrow cell transplantation and bone marrow stimulation with granulocyte macrophage-colony stimulating factor: Phase I/II clinical trial. *STEM CELLS* 2007;25:2066–2073.

42 Misra V, Lal A, El Khoury R et al. Intra-arterial delivery of cell therapies for stroke. *Stem Cells Dev* 2012;21:1007–1015.

43 Rosado-de-Castro PH, Pimentel-Coelho PM, da Fonseca LM et al. The rise of cell therapy

trials for stroke: Review of published and registered studies. *Stem Cells Dev* 2013;22:2095–2111.

44 Jin HJ, Park SK, Oh W et al. Down-regulation of CD105 is associated with multilineage differentiation in human umbilical cord blood-derived mesenchymal stem cells. *Biochem Biophys Res Commun* 2009;381:676–681.

45 Jung S, Panchalingam KM, Rosenberg L et al. Ex vivo expansion of human mesenchymal stem cells in defined serum-free media. *Stem Cells Int* 2012;2012:123030.

46 Mills JC, Stone NL, Pittman RN. Extracellular apoptosis. The role of the cytoplasm in the execution phase. *J Cell Biol* 1999;146:703–708.



See www.StemCellsTM.com for supporting information available online.